

**Research Article**

Effect of spring mid-support condition on the vibrations of the axially moving string

Saim Kural ^{a,*} 

^aManisa Celal Bayar University, Faculty of Engineering, Department of Mechanical Engineering, 45140, Yunusemre, Manisa, Turkey

ARTICLE INFO*Article history:*

Received 24 June 2020

Revised 29 August 2020

Accepted 05 September 2020

Keywords:

Axially moving string

Perturbation method

Spring supported string

Vibration analysis

ABSTRACT

In this study, the axially moving string with spring-loaded middle support is discussed. The supports assumed as simple support on the string both ends. The intermediate support shows the characteristics of the spring. The string velocity is accepted as harmonically varying around a mean value. The Hamiltonian principle is used to find the equations of motion. The equations of motion become nonlinear, considering the nonlinear effects caused by string extensions. The equations of motion and boundary conditions are become dimensionless by nondimensionalization. Approximate solutions were found by using multiple time scales which is one of the perturbation methods. By solving the linear problem that is obtained by the first terms of the perturbation series, the exact natural frequencies were calculated for the different locations of the mid-support, various spring coefficients, and various axial velocity values. The second-order nonlinear terms reveal the correction terms for the linear problem. Stability analysis is carried out for cases where the velocity change frequency is away from zero and two times the natural frequency. Stability boundaries are determined for the principal parametric resonance case.

© 2020, Advanced Researches and Engineering Journal (IAREJ) and the Author(s).

1. Introduction

Because of their low bending stiffness, products such as paper sheets, plastic films, power transmission belts, magnetic tapes, and textile fibers can be modeled as an axially moving string. Determining the dynamic behavior of these systems is very important for a stable and durable design. Fundamental studies about the subject can be found in references [1-3]. Wickert investigated the response problem for the vibration of an axially moving string that resting on an elastic foundation [4]. Nayfeh et al. [5] investigated solutions for quadratic and cubic nonlinearity problem and they concluded that the direct-perturbation method is better for these problems. Pellicano and Zirilli [6] have researched axially moving beam vibrations under nonlinear effects. The string-beam transition problem was investigated in [7] for axially moving media. An axially moving string with various non-ideal boundary conditions under nonlinear effects are investigated in [8]. Pellicano analyzed the dynamic properties of axially moving systems to explain the

complex dynamic behavior observed in experimental and numerical research [9].

Also, Bağdatlı et al. investigated continuous media as an axially moving beam with middle support [10]. The combined longitudinal-transverse nonlinear dynamics of an axially moving beam were described in Ghayesh et al. [11] and they discussed the stability of an axially moving beam that has middle spring support. Two dimensional movements of an axially moving string were described in [12]. Similarly, the moving string system is modeled by using Hamilton's principle [13]. An experimental study of the nonlinear characteristics of an axially moving string investigated in [14]. An alternative analytical method was investigated in [15] for the nonlinear vibration behavior of conical cantilever beams. To reduce vibration for a nonlinear drilling system a boundary control scheme was studied by He [16]. A new mathematical model studied in [17] to determine dynamic behavior for a beam or strip moving in a certain axial direction along a given area. Chen et al. [18] studied a nonlinear equation describing the transverse vibration of an axially moving string with

* Corresponding author. Tel.: +90 236 201 2380.

E-mail addresses: saimkural@gmail.com

ORCID: 0000-0003-1722-6252

DOI: 10.35860/iarej.757503

constant and time-dependent length. Zhao et al. [19] discussed the global balancing of an axially moving system under the input saturation nonlinearity circumstances. Zhang et al. [20] present numerical simulations for vibration reduction. Yilmaz et al. [21] used vibration analysis with FFT for determine the misalignment fault detection.

In this study, the effect of spring mid-support condition on the nonlinear vibrations of the axially moving string was discussed. The equations of motion were obtained by using the Hamiltonian principle. To solve the equations of motion; multiple time scale perturbation method was used. This method is a semi-analytical method used to obtain approximate solutions of systems with differential equations that are difficult or impossible to solve. Natural frequency analysis was performed depending on spring constant, string velocity, and position of the center support and the obtained results are given in graphics. Considering the effects of string elongation, the system became nonlinear, and then, the solution of the equations of motion was discussed. The effects of nonlinearities on solutions were investigated. The different vibration structures for different states of the string velocity change frequency are examined. By making stability analysis was made and the stable and unstable areas were identified.

2. The Equations of Motion and Solution

Figure 1 shows the basic model of the axially moving string with mid-supported spring. x^* , z^* and t^* are coordinate and time variables, respectively. w^* is the transverse and u^* is axial displacement, and v^* is the axial string velocity. In this section, the equations of motion were derived for axially moving spring mid-supported strings. Both ends were defined as simple-supported.

The Lagrangian for the system can be written the extended form of Hamiltonian Principle as:

$$\begin{aligned} \mathcal{L} = T - V = & \frac{1}{2} \rho A \int_0^{x_s} \{(\dot{w}_1^* + w_1^{*'} v^*)^2 \\ & + (v^* + \dot{u}_1^* + u_1^{*'} v^*)^2\} dx^* \\ & + \frac{1}{2} \rho A \int_{x_s}^L \{(\dot{w}_2^* + w_2^{*'} v^*)^2 \\ & + (v^* + \dot{u}_2^* + u_2^{*'} v^*)^2\} dx^* \\ & - \frac{1}{2} EA \int_0^{x_s} \left(u_1^{*'} + \frac{1}{2} w_1^{*'}{}^2\right)^2 dx^* \\ & - \frac{1}{2} EA \int_{x_s}^L \left(u_2^{*'} + \frac{1}{2} w_2^{*'}{}^2\right)^2 dx^* \\ & - \int_0^{x_s} P \left(u_1^{*'} + \frac{1}{2} w_1^{*'}{}^2\right) dx^* \\ & - \int_{x_s}^L P \left(u_2^{*'} + \frac{1}{2} w_2^{*'}{}^2\right) dx^* \\ & - \int k w_1^* dx^* @ x = x_s \end{aligned} \tag{1}$$

where $(\dot{\quad})$ means time derivative $\left(\frac{d}{dt^*}\right)$ and $(\quad)'$ means coordinate variable derivative $\left(\frac{d}{dx^*}\right)$. Euler-Bernoulli beam theory was used to obtain Equation (1). In this equation, the first two integrals on the right-hand side are kinetic energy between supports, the next four integrals are elastic potential energy due to elongation, and axial force (P), and last term is spring potential energy on mid-support location(x_s). After using the Hamiltonian principle into Equation (1), that can be expressed as follows:

$$\begin{aligned} & \rho A (\ddot{w}_{1,2}^* + 2\dot{w}_{1,2}^{*'} v^* + w_{1,2}^{*'} \dot{v}^* + w_{1,2}^{*''} v^{*2}) \\ & - EA \left(u_{1,2}^{*''} w_{1,2}^{*'} + u_{1,2}^{*'} w_{1,2}^{*''} + \frac{3}{2} w_{1,2}^{*'}{}^2 w_{1,2}^{*''}\right) \\ & - P w_{1,2}^{*''} = 0 \end{aligned} \tag{2}$$

$$\begin{aligned} & \rho A (\ddot{u}_{1,2}^* + 2\dot{u}_{1,2}^{*'} v^* + u_{1,2}^{*'} \dot{v}^* + \dot{v}^* + u_{1,2}^{*''} v^{*2}) \\ & - EA \left(u_{1,2}^{*'} + \frac{1}{2} w_{1,2}^{*'}{}^2\right)' = 0 \end{aligned} \tag{3}$$

$$\begin{aligned} & \rho A v^{*2} [w_1^{*'}(x_s) - w_2^{*'}(x_s)] - EA [u_1'(x_s) w_1'(x_s) + \\ & \frac{1}{2} w_1'^3(x_s) - u_2'(x_s) w_2'(x_s) - \frac{1}{2} w_2'^3(x_s)] - \\ & P [w_1^{*'}(x_s) - w_2^{*'}(x_s)] - k w_1(x_s) = 0 \end{aligned} \tag{4}$$

$$\begin{aligned} & \rho A v^{*2} [u_1'(x_s) - u_2'(x_s)] - EA [u_1'(x_s) - u_2'(x_s) + \\ & \frac{1}{2} w_1'^2(x_s) - \frac{1}{2} w_2'^2(x_s)] = 0 \end{aligned} \tag{5}$$

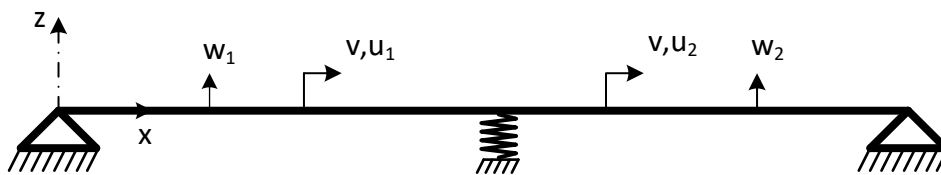


Figure 1. Axially moving string with intermediate spring support

Equations (2) and (3) obtained from double integrals and Equations (4) and (5) from single integrals. To simplify the future parametric analysis, let us define the dimensionless parameters as follows,

$$v_b^2 = \frac{EA}{P}, v_k = \frac{kL}{P}, \eta = \frac{x_s^*}{L}, x = \frac{x^*}{L}, t = \frac{t^*}{\sqrt{\frac{\rho AL^2}{P}}} \tag{6}$$

$$w_{1,2} = \frac{w_{1,2}^*}{L}, u_{1,2} = \frac{u_{1,2}^*}{L}, v = \frac{v^*}{\sqrt{\frac{P}{\rho A}}} \tag{7}$$

After all the operations were done and the necessary simplifications were made, the equations of motion and boundary conditions are obtained as follows,

$$(\ddot{w}_{1,2} + 2\dot{w}'_{1,2}v + w'_{1,2}\dot{v}) + w''_{1,2}(v^2 - 1) = \frac{1}{2}v_b^2 \left[\int_0^\eta w_1'^2 dx + \int_\eta^1 w_2'^2 dx \right] w''_{1,2} \tag{7}$$

$$w_1(0, t) = 0, w_2(1, t) = 0$$

$$w_1(\eta, t) =$$

$$\frac{1}{v_k} \left\{ 1 + \frac{1}{2}v_b^2\varepsilon \left[\int_0^\eta w_1'^2 dx + \int_\eta^1 w_2'^2 dx \right] \right\} (w_2'(\eta, t) - w_1'(\eta, t)) \tag{8}$$

The right-hand side of the Equation (7) represents the nonlinear terms from string elongation. $\ddot{w}_{1,2}$ represents local, $2\dot{w}'_{1,2}v$ represents Coriolis, and $v_b^2 w''_{1,2}$ represents centripetal acceleration. η is the location of center spring. The displacement in Equations (7) and (8) can be assumed as $w_{1,2} = \sqrt{\varepsilon} y_{1,2}$ ($\varepsilon \ll 1$) to ensure that the displacement due to nonlinear effects appear in the higher-order in perturbation method. Also, the string velocity can be assumed as varying harmonically around a fixed average value,

$$v = v_0 + \varepsilon v_1 \sin \Omega t \tag{9}$$

Thus, the equations of motion and boundary conditions are,

$$\ddot{y}_{1,2} + 2\dot{y}'_{1,2}v_0 + 2\dot{y}'_{1,2}\varepsilon v_1 \sin \Omega t + y'_{1,2}\varepsilon v_1 \Omega \cos \Omega t + (v_0^2 + \varepsilon^2 v_1^2 \sin^2 \Omega t + 2\varepsilon v_0 v_1 \sin \Omega t - 1)y''_{1,2} = \frac{1}{2}v_b^2\varepsilon \left[\int_0^\eta y_1'^2 dx + \int_\eta^1 y_2'^2 dx \right] y''_{1,2} \tag{10}$$

$$y_1(0, t) = 0, y_2(1, t) = 0$$

$$y_1(\eta, t) = \frac{1}{v_k} \left\{ 1 + \frac{1}{2}v_b^2\varepsilon \left[\int_0^\eta y_1'^2 dx + \int_\eta^1 y_2'^2 dx \right] \right\} (y_2'(\eta, t) - y_1'(\eta, t)) \tag{11}$$

3. Perturbation Analysis

For approximate solutions of Equation (10), multiple scales perturbation method was used. The displacement functions can be expanded as,

$$y_1(x, t; \varepsilon) = y_{11}(x, T_0, T_1) + \varepsilon y_{12}(x, T_0, T_1) + \dots \tag{12}$$

$$y_2(x, t; \varepsilon) = y_{21}(x, T_0, T_1) + \varepsilon y_{22}(x, T_0, T_1) + \dots \tag{13}$$

where $T_0=t$ is the slow, $T_1=\varepsilon t$ is the fast time scales, and time derivatives can be explained as follows:

$$\frac{d}{dt} = D_0 + \varepsilon D_1 + \dots, \frac{d^2}{dt^2} = D_0^2 + 2\varepsilon D_0 D_1 + \dots \tag{14}$$

where $D_n = d/dT_n$ Substituting Equations (12), (13), and (14) into Equation (10) yields,

The left-hand side ($0 < x_s < \eta$)

$$(D_0^2 + 2\varepsilon D_0 D_1)(y_{11} + \varepsilon y_{12}) + 2v_0(D_0 + \varepsilon D_1)(y'_{11} + \varepsilon y'_{12}) + (v_0^2 - 1)(y''_{11} + \varepsilon y''_{12}) + \varepsilon(2v_1 \sin \Omega T_0 (D_0 + \varepsilon D_1)(y'_{11} + \varepsilon y'_{12}) + 2v_0 v_1 \sin \Omega T_0 (y''_{11} + \varepsilon y''_{12}) + v_1 \Omega \cos \Omega T_0 (y'_{11} + \varepsilon y'_{12})) + \varepsilon^2 v_1^2 \sin^2 \Omega T_0 (y''_{11} + \varepsilon y''_{12}) = \frac{1}{2}v_b^2\varepsilon \left[\int_0^\eta (y'_{11} + \varepsilon y'_{12})^2 dx + \int_\eta^1 (y'_{21} + \varepsilon y'_{22})^2 dx \right] (y''_{11} + \varepsilon y''_{12}) \tag{15}$$

The right-hand side ($\eta < x_s < 1$)

$$\begin{aligned}
 & (D_0^2 + 2\varepsilon D_0 D_1)(y_{21} + \varepsilon y_{22}) \\
 & + 2v_0(D_0 + \varepsilon D_1)(y'_{21} + \varepsilon y'_{22}) \\
 & + (v_0^2 - 1)(y''_{21} + \varepsilon y''_{22}) \\
 & + \varepsilon(2v_1 \sin \Omega T_0 (D_0 + \varepsilon D_1)(y'_{21} + \varepsilon y'_{22}) \\
 & + 2v_0 v_1 \sin \Omega T_0 (y''_{21} + \varepsilon y''_{22}) \\
 & + v_1 \Omega \cos \Omega T_0 (y'_{21} + \varepsilon y'_{22})) \\
 & + \varepsilon^2 v_1^2 \sin^2 \Omega T_0 (y''_{21} + \varepsilon y''_{22}) \\
 & = \frac{1}{2} v_b^2 \varepsilon \left[\int_0^\eta (y'_{11} + \varepsilon y'_{12})^2 dx \right. \\
 & \left. + \int_\eta^1 (y'_{21} + \varepsilon y'_{22})^2 dx \right] (y''_{21} + \varepsilon y''_{22})
 \end{aligned} \tag{16}$$

If we make order arrangement to these equations and neglect the higher-order terms;

Order (1)

The equations of motion,

$$\begin{aligned}
 D_0^2 y_{11} + 2v_0 D_0 y'_{11} + (v_0^2 - 1)y''_{11} &= 0 \\
 D_0^2 y_{21} + 2v_0 D_0 y'_{21} + (v_0^2 - 1)y''_{21} &= 0
 \end{aligned} \tag{17}$$

And boundary conditions,

$$\begin{aligned}
 y_{12}(0, t) = 0, y_{22}(1, t) = 0, y_{12}(\eta, t) = y_{22}(\eta, t), \\
 y_{11}(\eta, t) = \frac{1}{v_k} [y'_{21}(\eta, t) - y'_{11}(\eta, t)]
 \end{aligned} \tag{18}$$

Order (ε)

The equations of motion,

$$\begin{aligned}
 & D_0^2 y_{12} + 2v_0 D_0 y'_{12} + (v_0^2 - 1)y''_{12} \\
 & = -2D_0 D_1 y_{11} - 2v_0 D_1 y'_{11} - 2v_1 \sin \Omega T_0 D_0 y'_{11} \\
 & - 2v_0 v_1 \sin \Omega T_0 y''_{11} - v_1 \Omega \cos \Omega T_0 y'_{11} \\
 & + \frac{1}{2} v_b^2 \left[\int_0^\eta y'_{11}{}^2 dx + \int_\eta^1 y'_{21}{}^2 dx \right] y''_{11} \\
 & D_0^2 y_{22} + 2v_0 D_0 y'_{22} + (v_0^2 - 1)y''_{22} \\
 & = -2D_0 D_1 y_{21} - 2v_0 D_1 y'_{21} - 2v_1 \sin \Omega T_0 D_0 y'_{21} \\
 & - 2v_0 v_1 \sin \Omega T_0 y''_{21} - v_1 \Omega \cos \Omega T_0 y'_{21} \\
 & + \frac{1}{2} v_b^2 \left[\int_0^\eta y'_{11}{}^2 dx + \int_\eta^1 y'_{21}{}^2 dx \right] y''_{21}
 \end{aligned} \tag{19}$$

And boundary conditions,

$$\begin{aligned}
 y_{12}(0, t) = 0, y_{22}(1, t) = 0, \\
 y_{12}(\eta, t) = y_{22}(\eta, t), \\
 y_{12}(\eta, t) = \frac{1}{2} v_b^2 \left[\int_0^\eta y_1'^2 dx \right. \\
 \left. + \int_\eta^1 y_2'^2 dx \right] y_{11}(\eta, t)
 \end{aligned} \tag{20}$$

We can get the solution function for the linear order (O(1)),

$$\begin{aligned}
 y_{11}(x, T_0, T_1; \varepsilon) &= A_n(T_1) e^{i\omega_n T_0} Y_1(x) \\
 &+ \bar{A}_n(T_1) e^{-i\omega_n T_0} \bar{Y}_1(x) \\
 y_{21}(x, T_0, T_1; \varepsilon) &= A_n(T_1) e^{i\omega_n T_0} Y_2(x) \\
 &+ \bar{A}_n(T_1) e^{-i\omega_n T_0} \bar{Y}_2(x)
 \end{aligned} \tag{21}$$

Substituting Equations (21) into Equation (17), one obtains,

$$\begin{aligned}
 (v_0^2 - 1)Y_1'' + 2iv_0 \omega_n Y_1' - \omega_n^2 Y_1 &= 0 \\
 (v_0^2 - 1)Y_2'' + 2iv_0 \omega_n Y_2' - \omega_n^2 Y_2 &= 0
 \end{aligned} \tag{22}$$

and boundary conditions,

$$\begin{aligned}
 Y_1(0, t) = 0, Y_2(1, t) = 0, Y_1(\eta, t) = Y_2(\eta, t), \\
 Y_1(\eta, t) = \frac{1}{v_k} [Y_2'(\eta, t) - Y_1'(\eta, t)]
 \end{aligned} \tag{23}$$

For the approximate solution, the following functions are proposed,

$$\begin{aligned}
 Y_1(x) &= c_1 e^{\beta_1 x} + c_2 e^{\beta_2 x} \\
 Y_2(x) &= c_3 e^{\beta_1 x} + c_4 e^{\beta_2 x}
 \end{aligned} \tag{24}$$

By applying boundary conditions, a matrix is created with obtained four equations. By taking the determinant of this matrix, the frequency equation obtained in a general form as follows.

$$\begin{aligned}
 & \frac{1}{2} \{-2(e^{\eta\beta_1} - e^{\eta\beta_2})(e^{\eta\beta_1 + \beta_2} - e^{\beta_1 + \eta\beta_2})v_k \\
 & + e^{\eta(\beta_1 + \beta_2)}(e^{\beta_1} - e^{\beta_2})(\beta_1 - \beta_2)\} \\
 & = 0
 \end{aligned} \tag{25}$$

The natural frequencies against mean velocity (v_0) and spring coefficient (v_k) are given in the following figures. Figure 2 was obtained for the middle support at the $\mu = 0.1$ location. The variations of v_k between 0 and 30, and v_0 between 0 and 1 were examined. Natural frequencies drop to zero while mean velocity increasing. The natural frequencies increase directly proportional to v_k . The effect of the spring coefficient on the natural frequencies decreases as the mean velocity increases.

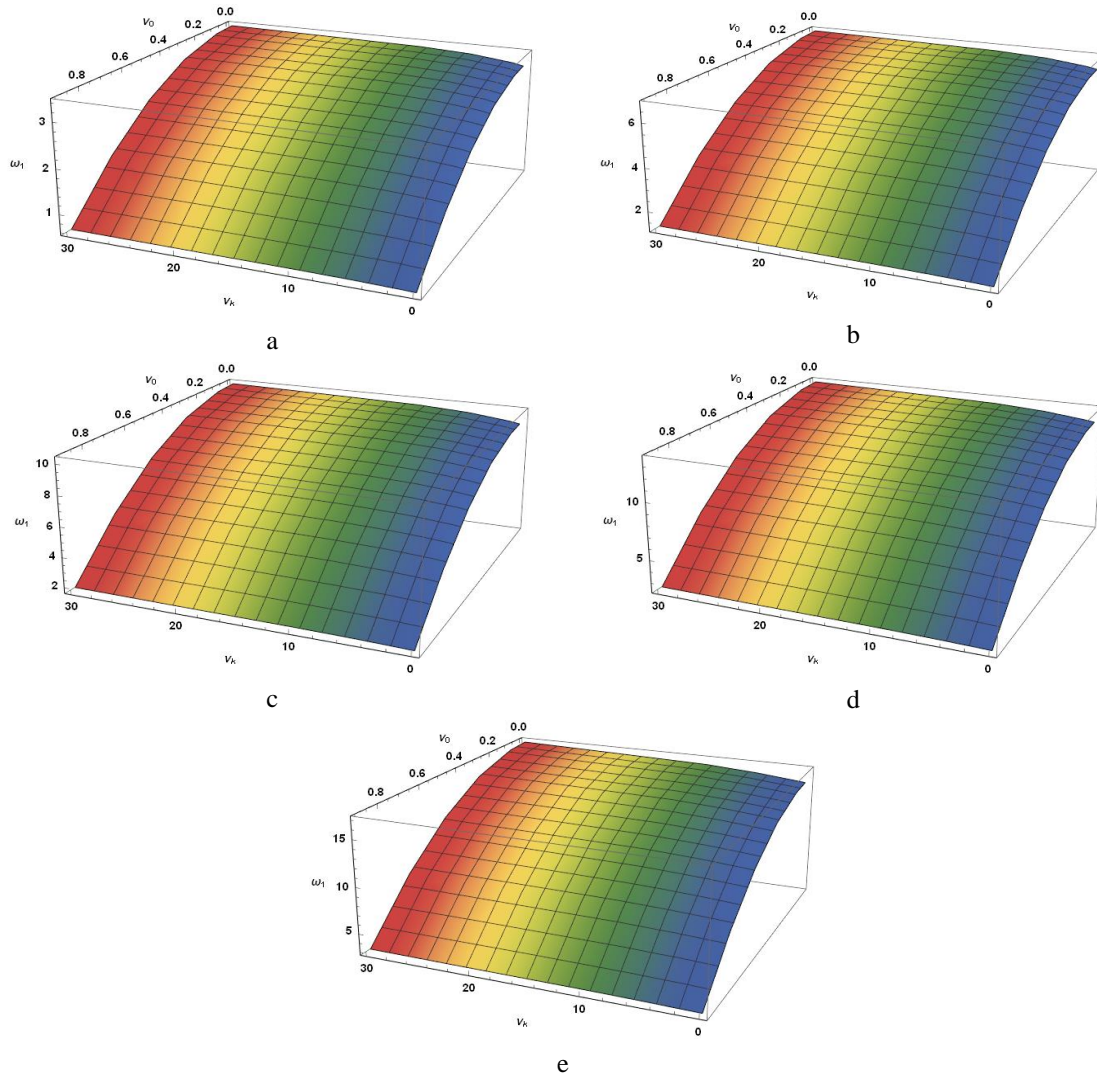


Figure 2. Variation of the natural frequency values with axial velocity and spring coefficient ($\mu = 0.1$ location) (a; first mode, b; second mode, c; third mode, d; fourth mode, e; fifth mode)

The first natural frequencies for $\mu = 0.1$, $\mu = 0.3$ and $\mu = 0.5$ locations compared in Figure 3. As expected $\mu = 0.1$ location has the smallest natural frequency values, and $\mu = 0.5$ location has the highest. When $v_k = 0$ all 3 locations have the same values. While v_0 increases the effect of the

spring coefficient on the natural frequency values decreases, again. In Figure 2 all five natural frequency shapes are similar, but for $\mu = 0.3$ and $\mu = 0.5$ positions v_k has more effect on natural frequency.

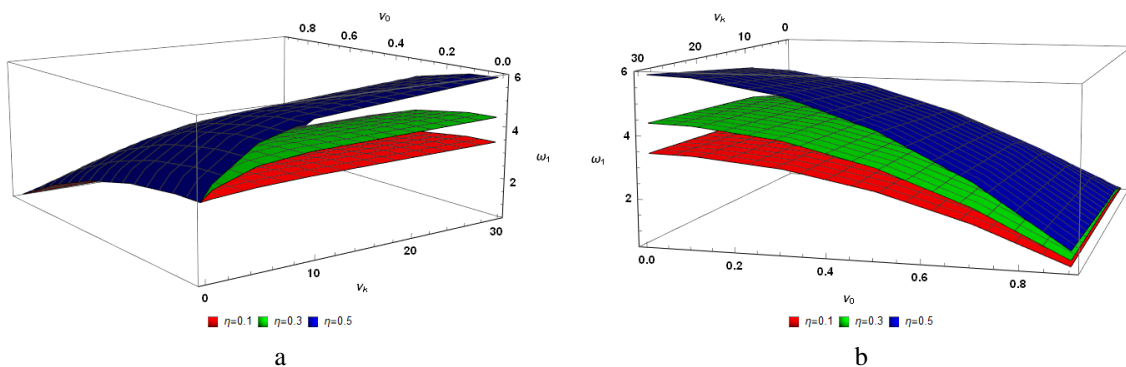


Figure 3. Comparison of the first mode natural frequency values for different μ locations (a; left-hand side, b; right-hand side)

We can get the solution function for the linear order (O(1));

$$\begin{aligned}
 y_{12}(x, T_0, T_1) &= \phi_1(x, T_1)e^{i\omega_n T_0} \\
 &+ W_1(x, T_0, T_1) + c.c. \\
 y_{22}(x, T_0, T_1) &= \phi_2(x, T_1)e^{i\omega_n T_0} \\
 &+ W_2(x, T_0, T_1) + c.c.
 \end{aligned}
 \tag{26}$$

The first term (ϕ) refers to the secular terms of the function, the second term (W) to the non-secular terms of the function, and last term (c.c.) means complex conjugate.

$$\begin{aligned}
 \cos \Omega T_0 &= \frac{e^{i\Omega T_0} + e^{-i\Omega T_0}}{2} \\
 \sin \Omega T_0 &= \frac{e^{i\Omega T_0} - e^{-i\Omega T_0}}{2i}
 \end{aligned}
 \tag{27}$$

Following equations are obtained by doing above trigonometric transformations and write them together with the proposed solutions to the nonlinear order equations,

$$\begin{aligned}
 e^{i\omega_n T_0} &[-\omega_n^2 \phi_1 + 2iv_0 \omega_n \phi_1' + (v_0^2 - 1)\phi_1''] = \\
 &-2(i\omega_n Y_1 + v_0 Y_1') A' e^{i\omega_n T_0} \\
 &+ v_1 \left(-\omega_n Y_1' - \frac{\Omega}{2} Y_1' + iv_0 Y_1''\right) A e^{i(\Omega + \omega_n) T_0} \\
 &+ v_1 \left(\omega_n \bar{Y}_1' - \frac{\Omega}{2} \bar{Y}_1' + iv_0 \bar{Y}_1''\right) \bar{A} e^{i(\Omega - \omega_n) T_0} \\
 &+ \frac{1}{2} v_b \left[\begin{aligned} &2Y_1'' \left(\int_0^\eta Y_1' \bar{Y}_1' dx + \int_\eta^1 Y_2' \bar{Y}_2' dx \right) \\ &+ \bar{Y}_1'' \left(\int_0^\eta Y_1'^2 dx + \int_\eta^1 Y_2'^2 dx \right) \end{aligned} \right] A^2 \bar{A} e^{i\omega_n T_0} \\
 &+ N.S.T. + c.c.
 \end{aligned}
 \tag{28}$$

$$\begin{aligned}
 e^{i\omega_n T_0} &[-\omega_n^2 \phi_2 + 2iv_0 \omega_n \phi_2' + (v_0^2 - 1)\phi_2''] = \\
 &-2(i\omega_n Y_2 + v_0 Y_2') A' e^{i\omega_n T_0} \\
 &+ v_1 \left(-\omega_n Y_2' - \frac{\Omega}{2} Y_2' + iv_0 Y_2''\right) A e^{i(\Omega + \omega_n) T_0} \\
 &+ v_1 \left(\omega_n \bar{Y}_2' - \frac{\Omega}{2} \bar{Y}_2' + iv_0 \bar{Y}_2''\right) \bar{A} e^{i(\Omega - \omega_n) T_0} \\
 &+ \frac{1}{2} v_b \left[\begin{aligned} &2Y_2'' \left(\int_0^\eta Y_1' \bar{Y}_1' dx + \int_\eta^1 Y_2' \bar{Y}_2' dx \right) \\ &+ \bar{Y}_2'' \left(\int_0^\eta Y_1'^2 dx + \int_\eta^1 Y_2'^2 dx \right) \end{aligned} \right] A^2 \bar{A} e^{i\omega_n T_0} \\
 &+ N.S.T. + c.c.
 \end{aligned}
 \tag{29}$$

$$\begin{aligned}
 \phi_1(0) &= 0, \phi_2(1) = 0, \\
 \phi_1(\eta) &= \phi_2(\eta) \\
 \phi_1(\eta) &= \frac{1}{2} v_b \left[\begin{aligned} &2Y_1(\eta) \left(\int_0^\eta Y_1' \bar{Y}_1' dx + \int_\eta^1 Y_2' \bar{Y}_2' dx \right) \\ &+ \bar{Y}_1(\eta) \left(\int_0^\eta Y_1'^2 dx + \int_\eta^1 Y_2'^2 dx \right) \end{aligned} \right] A^2 \bar{A}
 \end{aligned}
 \tag{30}$$

The different vibration structures for different states of the string velocity change frequency (Ω) are examined separately below.

i) Ω ; away from $2\omega_n$ and 0:

In this case, the solvability condition is obtained from Equations (28) and (29) as follows.

$$D_1 A - k_3 A^2 \bar{A} = 0
 \tag{31}$$

The amplitude A can be defined as follows,

$$A = \frac{1}{2} a_n e^{i\theta}
 \tag{32}$$

Inserting Equation (32) into Equation (31) and separate the real and imaginary parts.

where k_3 is;

$$\begin{aligned}
 k_3 &= \frac{1}{4} v_b^2 \left(\frac{2 \left(\int_0^\eta Y_1' \bar{Y}_1' dx + \int_\eta^1 Y_2' \bar{Y}_2' dx \right) \left(\int_0^\eta Y_1'' \bar{Y}_1 dx + \int_\eta^1 Y_2'' \bar{Y}_2 dx \right)}{i\omega_n \left(\int_0^\eta Y_1 \bar{Y}_1 dx + \int_\eta^1 Y_2 \bar{Y}_2 dx \right) + v_0 \left(\int_0^\eta Y_1' \bar{Y}_1 dx + \int_\eta^1 Y_2' \bar{Y}_2 dx \right)} \right. \\
 &+ \left. \frac{\left(\int_0^\eta Y_1'^2 dx + \int_\eta^1 Y_2'^2 dx \right) \left(\int_0^\eta \bar{Y}_1'' \bar{Y}_1 dx + \int_\eta^1 \bar{Y}_2'' \bar{Y}_2 dx \right)}{i\omega_n \left(\int_0^\eta Y_1 \bar{Y}_1 dx + \int_\eta^1 Y_2 \bar{Y}_2 dx \right) + v_0 \left(\int_0^\eta Y_1' \bar{Y}_1 dx + \int_\eta^1 Y_2' \bar{Y}_2 dx \right)} \right)
 \end{aligned}
 \tag{33}$$

$$\begin{aligned} a_n' &= 0 \\ \theta' &= \frac{1}{4} k_{3I} a_n^2 \end{aligned} \quad (34)$$

Hence,

$$\begin{aligned} a_n &= a_{0n} \text{ (a is continuous)} \\ \theta &= \frac{1}{4} k_{3I} a_{0n}^2 T_1 + \theta_0 \end{aligned} \quad (35)$$

The real part of k_3 is small enough to be neglected compared to its imaginary part.

$$k_3 = ik_{3I} \quad (36)$$

Nonlinear frequency equation from here,

$$(\omega_n)_{nl} = \omega_n + \varepsilon \frac{1}{4} k_{3I} a_{0n}^2 \quad (37)$$

The relationship between nonlinear natural frequency and amplitudes is shown in Figures. 4 to 7. The effect of the axial mean velocity for the first mode is shown in Figs 6 and 7 for $\mu = 0.3$ and $\mu = 0.5$, respectively. These comparisons are again shown for $v_k = 1$ in Fig. 8 and for the second mode in Fig. 9. Nonlinearities increase directly proportional to mean velocity. When v_k increase, nonlinearity decreases. When the mid-spring location is at $\mu = 0.5$, nonlinearity is increase according to $\mu = 0.3$.

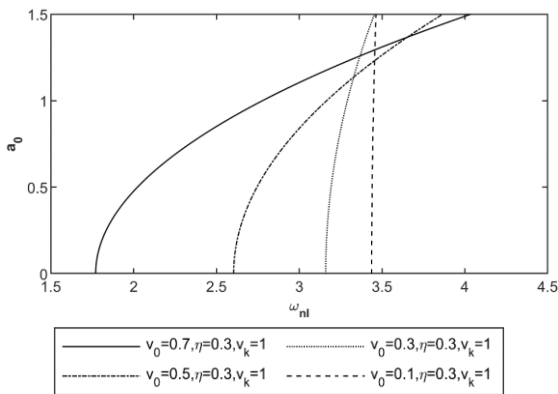


Figure 4. Nonlinear frequency-amplitude variation for axial mean velocity (mode 1).

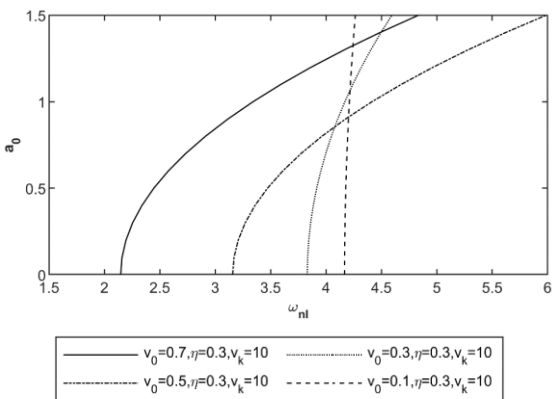


Figure 5. Nonlinear frequency-amplitude variation for axial mean velocity (mode 1).

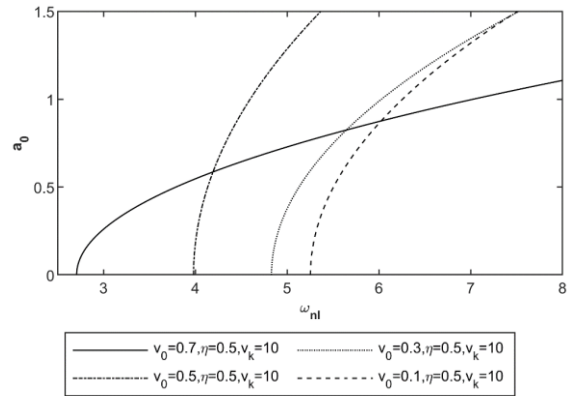


Figure 6. Nonlinear frequency-amplitude variation for axial mean velocity (mode 1).

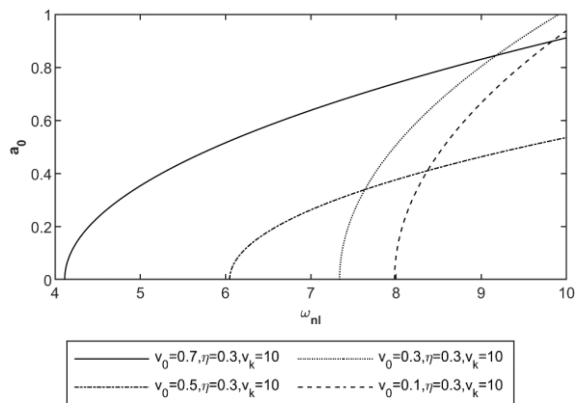


Figure 7. Variation of the amplitude with nonlinear frequency values for axial velocity (mode 2).

ii) *Principal parametric resonance:*

In this case, the velocity change frequency can be defined as follows;

$$\Omega = 2\omega_n + \varepsilon\sigma \quad (38)$$

From Equations. (28) and (29) solubility condition is obtained as follows

$$D_1 A + k_0 \bar{A} e^{i\sigma T_1} - k_3 A^2 \bar{A} = 0 \quad (39)$$

By inserting the amplitude definition in Equation (39) and divide it into real and imaginary parts.

$$\begin{aligned} a'_n &= a_n(k_{0I} \sin\gamma_n - k_{0R} \cos\gamma_n) \\ \gamma'_n &= \sigma + 2(k_{0R} \sin\gamma_n + k_{0I} \cos\gamma_n) - \frac{1}{2} k_{3I} a_n^2 \quad (40) \\ k_0 &= k_{0R} + ik_{0I}, \gamma_n = \sigma T_1 - 2\theta_n \end{aligned}$$

For stable regime a'_n and γ'_n can be assumed zero and hence;

$$\sigma_1 = \frac{1}{2} k_{3I} a_n^2 - 2\sqrt{k_{0R}^2 + k_{0I}^2} \quad (41)$$

$$\sigma_2 = \frac{1}{2} k_{3I} a_n^2 + 2\sqrt{k_{0R}^2 + k_{0I}^2} \quad (42)$$

where k_0 is;

$$k_0 = \frac{1}{4} v_1 \frac{(\Omega - 2\omega_n) \left(\int_0^\eta \bar{Y}_1' \bar{Y}_1' dx + \int_\eta^1 \bar{Y}_2' \bar{Y}_2' dx \right) - 2iv_0 \left(\int_0^\eta \bar{Y}_1'' \bar{Y}_1 dx + \int_\eta^1 \bar{Y}_2'' \bar{Y}_2 dx \right)}{i\omega_n \left(\int_0^\eta Y_1 \bar{Y}_1 dx + \int_\eta^1 Y_2 \bar{Y}_2 dx \right) + v_0 \left(\int_0^\eta Y_1' \bar{Y}_1 dx + \int_\eta^1 Y_2' \bar{Y}_2 dx \right)} \quad (43)$$

We can write the complex amplitude in the form below (Equation (44)), inserting it into Equation (39) and divide it into real and virtual parts gives Equations (45) and (46);

$$A_n = \frac{1}{2} (p_n + iq_n) e^{i(\sigma T_1/2)} \quad (44)$$

$$p'_n = -k_{0R} p_n + \left(\frac{\sigma}{2} - k_{0I} \right) q_n - \frac{1}{4} k_{3I} q_n (p_n^2 + q_n^2) \quad (45)$$

$$= F_1(p_n, q_n)$$

$$q'_n = k_{0R} q_n - \left(\frac{\sigma}{2} + k_{0I} \right) p_n + \frac{1}{4} k_{3I} p_n (p_n^2 + q_n^2) \quad (46)$$

$$= F_2(p_n, q_n)$$

Hence the Jacobian matrix.

$$\begin{bmatrix} \partial F_1 / \partial p_n & \partial F_1 / \partial q_n \\ \partial F_2 / \partial p_n & \partial F_2 / \partial q_n \end{bmatrix}_{p_n=q_n=0} \quad (47)$$

and eigenvalues.

$$\lambda_{1,2} = \pm \sqrt{k_{0R}^2 + k_{0I}^2 - \frac{\sigma^2}{4}} \quad (48)$$

From here, the stability limits yields;

$$\sigma > 2\sqrt{k_{0R}^2 + k_{0I}^2}, \sigma < -2\sqrt{k_{0R}^2 + k_{0I}^2} \quad (49)$$

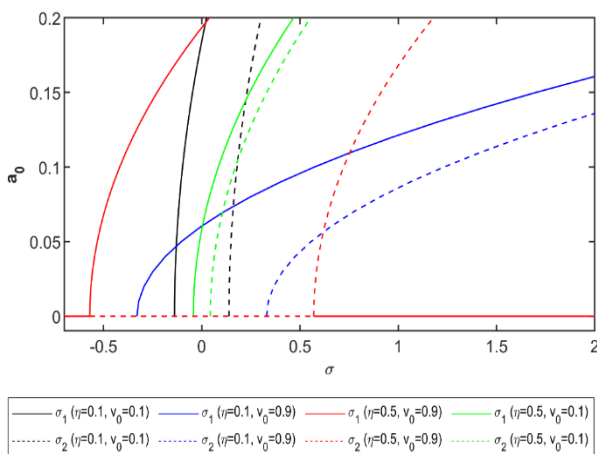


Figure 8. Variation of the aptitude with detuning parameter for different μ locations and axial velocity.

In Figure 10, the changes of amplitudes depending on the detuning parameter are given comparatively. The unstable region increases with the spring velocity increase. $\mu = 0.5$ has a smaller unstable region according to $\mu = 0.1$ for low spring velocities but while spring velocity increasing this unstable region increases much more according to case $\mu = 0.1$.

4. Conclusions

The transverse vibrations of an axially moving string with spring-loaded middle support are discussed. From this study, we can see there is no perfect design for all conditions. The design of Spring mid-supported string must be made specifically for the location where it will be used, and selections should be made according to the following criteria.

- Increasing rigidity of the spring coefficient also increases the natural frequency of the string.
- While the string velocity increasing, the natural frequency decrease.
- When mid-support moves right, natural frequencies increase more significantly with the rigidity of the spring coefficient increase until center location.
- When v_k increase, nonlinearity decreases.
- When the mid-spring location is at $\mu = 0.5$, nonlinearity is increase according to $\mu = 0.3$.
- The unstable region increases with the velocity increase.
- The unstable region is smaller for $\mu = 0.5$ according to $\mu = 0.1$ for smaller low spring velocities but while spring velocity increasing this unstable region increases much more for $\mu = 0.5$.

Declaration

The author(s) declared no potential conflicts of interest with respect to the research, authorship, and/or publication of this article. The author(s) also declared that this article is original, was prepared in accordance with international publication and research ethics, and ethical committee permission or any special permission is not required.

Nomenclature

- \mathcal{L} : Lagrangian.
- T : Kinetic energy.
- V : Potential energy.
- L : String Length.

ρ	: Constant density.
A	: Cross-section of string.
E	: Young's modulus.
v_b	: Longitudinal rigidity.
v_k	: The effect of the rigidity of the spring coefficient.
N.S.T.	: Non-secular terms.
σ	: The detuning parameter.

References

1. Thurman, A. L., Mote, C.D., *Free, Periodic, Nonlinear Oscillation of an Axially Moving Strip*. Journal of Applied Mechanics, 1969. **36**(1): p. 83-91.
2. Ulsoy, A.G., Mote, C.D. Jr., and Syzmani, R., *Principal developments in band saw vibration and stability research*. Holz als Roh- und Werkstoff, 1978. **36**(7): p. 273-280.
3. Wickert, J.A., Mote, C.D. Jr., *Current research on the vibration and stability of axially moving materials*. Shock and Vibration Digest, 1988. **20**(5): p. 3-13.
4. Wickert, J.A., *Response solutions for the vibration of a traveling string on an elastic foundation*. Journal of Vibration and Acoustics, 1994. **116**(1): p. 137-139.
5. Nayfeh, A.H., Nayfeh, J.F., Mook, D.T., *On methods for continuous systems with quadratic and cubic nonlinearities*. Nonlinear Dynamics, 1992. **3**: p. 145-162.
6. Pellicano, F., Zirilli, F., *Boundary layers and non-linear vibrations in an axially moving beam*. International Journal of Non-Linear Mechanics, 1998. **33**(4): p. 691-711.
7. Kural, S., Özkaya, E., *Vibrations of an axially accelerating, multiple supported flexible beam*. Structural Engineering and Mechanics, 2012. **44**(4): p. 521-538.
8. Yurddaş, A., Özkaya, E., Boyacı, H., *Nonlinear vibrations and stability analysis of axially moving strings having nonideal mid-support conditions*. Journal of Vibration and Control, 2012. **20**(4): p. 518-534.
9. Pellicano F., *On the dynamic properties of axially moving system*. Journal of Sound and Vibration, 2005. **281**(3-5): p. 593-609.
10. Bağdatlı, S.M., Özkaya, E., Öz, H.R., *Dynamics of Axially Accelerating Beams with an Intermediate Support*. Journal of Vibration and Acoustics, 2011. **133**(3): 031013, 10 pages.
11. Ghayesh, M. H., Amabili, M. Païdoussis, M. P., *Nonlinear vibrations and stability of an axially moving beam with an intermediate spring support: two-dimensional analysis*. Nonlinear Dynamics, 2012. **70**(1): p. 335-354.
12. Nguyen, Q. C., Hong, K.S., *Simultaneous control of longitudinal and transverse vibrations of an axially moving string with velocity tracking*. Journal of Sound and Vibration, 2012. **331**(13): p. 3006-3019.
13. He, W., Ge, S. S., Huang, D., *Modeling and vibration control for a nonlinear moving string with output constraint*. IEEE/ASME Transactions on Mechatronics, 2015. **20**(4): p. 1886-1897.
14. Xia, C., Wu, Y., Lu, Q., *Experimental study of the nonlinear characteristics of an axially moving string*. Journal of Vibration and Control, 2015. **21**(16): p. 518-534.
15. Sun, W., Sun, Y., Yu, Y., Zheng, S., *Nonlinear vibration analysis of a type of tapered cantilever beams by using an analytical approximate method*. Structural Engineering and Mechanics, 2016. **59**(1): p. 1-14.
16. He, W., Nie, S., Meng, T., Liu, Y.-J., *Modeling and vibration control for a moving beam with application in a drilling riser*. IEEE Transactions on Control Systems Technology, 2017. **25**(3): p. 1036-1043.
17. Vetyukov, Y., *Non-material finite element modelling of large vibrations of axially moving strings and beams*. Journal of Sound and Vibration, 2018. **414**(3): p. 299-317.
18. Chen, E. , Li, M., Ferguson, N., Lu, Y., *An adaptive higher order finite element model and modal energy for the vibration of a traveling string*. Journal of Vibration and Control, 2018. **25**(5): p. 996-1007.
19. Zhao, Z., Ma, Y., Liu, G., Zhu, D., Wen, G., *Vibration Control of an Axially Moving System with Restricted Input*. Complexity, 2019. **2019**: Article ID 2386435, 10 pages.
20. Zhang, X., Pipeleers, G., Hengster-Movrić, K., Faria, C., *Vibration reduction for structures: distributed schemes over directed graphs*. Journal of Vibration and Control, 2019. **25**(14): p. 2025-2042.
21. Yılmaz, Ö , Aksoy, M , Kesilmiş, Z ., *Misalignment fault detection by wavelet analysis of vibration signals*. International Advanced Researches and Engineering Journal, 2019. **3**(3): p. 156-163.